

Microstructure and performance evaluations on Q&P hot stamping parts of several UHSS sheet metals

HAN XianHong¹, ZHONG YaoYao^{1,2}, TAN ShuLin¹, DING YaNan¹ & CHEN Jun^{1*}¹ Department of Plasticity Technology, Shanghai Jiao Tong University, Shanghai 200030, China;² SAIC Motor Technical Center, Shanghai 201804, China

Received October 13, 2016; accepted July 26, 2017; published online August 25, 2017

Hot stamping (press hardening) is widely used to fabricate safety components such as door beams and B pillars with increased strength via quenching. However, parts that are hot-stamped from ultra-high-strength steel (UHSS) have very limited elongation, i.e., low ductility. In the present study, a novel variant of hot stamping technology called quenching-and-partitioning (Q&P) hot stamping was developed. This approach was tested on several UHSS sheet metals, and it was confirmed that this method can be used to overcome the drawbacks associated with conventional hot stamping. The applicability of Q&P hot stamping to each of these steels was also assessed. The part properties and performances of three widely used ultra-high-strength sheet metals, B1500HS, 27SiMn, and TRIP780, were evaluated through tensile testing and microstructural observations. The results demonstrated that the ductility of Q&P hot-stamped sheet metals was notably higher than that of the conventionally hot-stamped parts because Q&P hot stamping gives rise to a dual-phase structure of both martensite and austenite. Further, material tests demonstrated that the Q&P treatment had positive effects on all three selected materials, of which TRIP780 had the best ductility and the highest value of the product of strength and plasticity. Scanning electron microscopy images indicated that the silicon in the steels could limit the formation of cementite and would, therefore, improve the mechanical properties of Q&P hot-stamped products.

ultra-high-strength steel, hot stamping, quenching and partitioning process, high ductility

Citation: Han X H, Zhong Y Y, Tan S L, et al. Microstructure and performance evaluations on Q&P hot stamping parts of several UHSS sheet metals. *Sci China Tech Sci*, 2017, 60: 1692–1701, doi: 10.1007/s11431-016-9111-y

1 Introduction

Hot stamping is widely used to produce ultra-high-strength steel parts. During the hot stamping process, a blank of boron steel is initially heated to approximately 900°C and held in the furnace for 3 to 5 min until it is fully austenitized. Then, the heated blank is quickly transferred to the stamping tool, and the forming process is immediately performed. Simultaneously, the quenching process takes place inside the tool, where cooling channels are integrated to ensure a suitable cooling rate. Thus, a high-strength product with good stamp-

ing precision is obtained after cooling to room temperature [1–3].

The strength of hot-stamped products reaches 1500 MPa or higher, which makes them popular in automotive manufacturing so as to increase the safety and decrease the weight of the vehicle. However, such hot stamping products usually have lower elongations of approximately 5% [1,4,5], which significantly reduces the ductility of the final products. The product of strength and plasticity (PSP), given as $\sigma_b \cdot A_t$ (where σ_b represents the tensile strength and A_t represents the total elongation), is used to represent the comprehensive performance of a mechanical part during energy absorption [6]. The PSPs of most hot-stamped parts produced today are less than

Corresponding author (email: jun_chen@sjtu.edu.cn)

10 GPa%, which meets the standards for only first-generation automotive sheet steels [7].

Higher PSPs can be attained by designing new materials that have higher percentage compositions of rare and precious metals; this is the manner in which second-generation steel is created. However, such steels are usually expensive, which is a barrier to widespread implementation in the automotive industry. Another approach to increase the PSP while controlling the material cost to an acceptable level is to integrate advanced heat treatments into the forming process. Introducing a tempering treatment after the hot stamping process can eliminate residual stress and can be used to attain different strengths and elongations by adjusting the tempering temperature [8,9]. It has also been shown that higher ductility can be achieved through a semi-hot stamping process, the process of which is similar to conventional hot stamping but uses a lower heating temperature; however, this method slightly decreases the strength of the material [10]. In addition, Naderi et al. [11] observed that the presence of ferrite phase induced by the use of a water-cooled punch can increase the PSP; this finding was further supported by Santofimia et al. [12] and Hao et al. [13].

Quenching and partitioning (Q&P) is a novel heat-treatment process presented by Speer et al. [14,15]. By Q&P, dual-phase microstructures of martensite and residual austenite can be formed, which notably improves the elongation of the material. Based on the Q&P process, Hsu et al. [16] proposed a new heat treatment, called the quenching-partitioning-tempering process, for designed steels containing carbide formation elements. In addition, Chen et al. [17] integrated deformation-induced ferrite transformation with the Q&P process (DIFT+Q&P) for low-carbon boron steels, achieving PSPs higher than 20 GPa% in all samples. Liu et al. [18,19] proposed to combine the Q&P treatment with hot stamping, creating a process called Q&P hot stamping (HS+Q&P); a thermal simulation of this process showed that the elongation of the final part significantly increases and the high strength of the material is retained. Han et al. [20,21] designed an experimental tool to perform the HS+Q&P process. Lin et al. [22] proposed a hot stamping/bake-toughening process, demonstrating that carbon partitioned from martensite to untransformed austenite, resulting in a PSP as high as 21.9 GPa%.

Currently, boron steels are widely used to produce ultra-high-strength parts via the hot stamping process. Various boron alloys have been developed and produced by different steel companies such as Usibor1500, 20MnB5, 22MnB5, 27MnCrB5, B1500HS, BR1500HS, WHT1300HF, among others. Some of them contain coatings and others do not; nevertheless, the chemical compositions of these steels are similar. On the contrary, most of the metals proposed for Q&P heat treatment in the published literature, including 0.35C-1.3Mn-0.74Si

wt% [14], 0.19C-1.61Mn-0.35Si-1.1Al-0.09P wt% [23], 0.28C-1.4Si-0.67Mn-1.49Cr-0.56Mo wt% [24], 0.41C-1.27Si-1.30Mn-1.01Ni-0.56Cr wt% [25], and 0.2C-1.40Si-1.80Mn wt% [26], are in the experimental stages and have not been mass produced.

In this study, a new Q&P hot stamping process was developed based on previous studies. An experimental U-cap stamping tool was introduced and a series of Q&P hot stamping trials were executed, and the results were compared with the results of conventional hot stamping. Three mass-produced and readily available steels, B1500HS, 27SiMn, and TRIP780, were used in this study; their performances during the Q&P process were evaluated using a thermal simulation machine, Gleeble3500.

2 Description of Q&P hot stamping process and experimental tool design

In the conventional hot stamping process, when the hot blank is moved to the cool tools, it undergoes forming and quenching as its temperature drops continuously toward room temperature. However, in Q&P hot stamping, when the elevated blank is moved into the tool, the forming and quenching processes simultaneously commence with hot stamping. Thus, the blank is not quenched to room temperature directly; rather, the temperature change is interrupted at a certain temperature called the quenching temperature (T_Q), which is between the temperatures at which the martensitic transformation begins (M_s) and ceases (M_f). Then, the blank is held at another temperature, called the partitioning temperature (T_P), for a fixed time interval, called the partitioning time (t_P). T_P can be greater than or equal T_Q ; when $T_P > T_Q$, the process is called a two-step Q&P hot stamping process and when $T_P = T_Q$, it is called a one-step Q&P hot stamping process (depicted in Figure 1). A previous study of 0.2C-1.53Si-1.46Mn steel by Zhong [27] showed that the ductility of steel after the two-step Q&P process is higher than that after the one-step Q&P process. However, the temperature of a sheet changes in a complicated way during the two-step process and can hardly be measured with the existing experimental tools. So, only the one-step Q&P hot stamping process was studied in this study.

Compared with the conventional hot stamping process, the partitioning stage was more pronounced in the Q&P hot stamping process. According to the results of a study of Speer et al. [14,15], the partitioning stage causes partitioning of supersaturated carbon from martensite to retained austenite, leading to carbon enrichment and austenite stabilization. Thus, the final part is composed of dual-phase microstructures containing both martensite and austenite, which is regarded as the main reason for the observed improvement in the elongation and PSP.

It is well accepted that cooling channels should be included

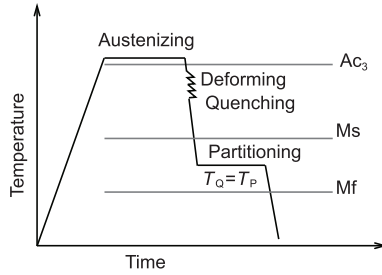


Figure 1 Schematic of the one-step Q&P hot stamping process.

in the conventional hot stamping tool to maintain it at a low temperature during the hot stamping process, thereby ensuring that the cooling rate of the steel is higher than a critical value. However, there are two quenching steps and one partitioning step during the Q&P hot stamping process; the temperature should rapidly decrease during the quenching processes but be maintained at an elevated value during the partitioning process. This requirement presents a unique challenge to the tool design. Figure 2 presents an experimental tool design for the Q&P hot stamping process, which was presented by the authors as a patent in 2015 [28]. Instead of the water-based cooling system used in conventional hot stamping tools, in this design, a heating system was integrated into the die and punch to increase the temperature of the tool to T_Q ; the high cooling rate required during the quenching step is provided by a blast system with cooling air. The tool is heated before the hot stamping process and kept at T_Q during the whole process. The cooling air is injected when the quenching step begins and then switched off at the start of the partitioning step. To allow the cooling air to pass through the bottom of the die into the cavity, a special porous plate was designed, as shown in Figure 3. The cooling effects can be controlled by using different porous plates with different hole densities and distributions. Although the tool shown in Figure 2 was designed for a U-cap part, the same principle can be applied to other parts.

The partitioning process can also be achieved outside of the tool as follows. First, the hot blank is put into a conventional hot stamping tool with cool channels to perform the forming and quenching processes until the temperature of the blank decreases to T_Q . At this time, the tool is opened and the formed part is quickly transferred into a furnace, which is kept at T_Q , to perform the partitioning process for a period of t_p . Then, the part is removed from the furnace to perform the second quenching process by water spraying or other methods. For this method, no changes to the conventional hot stamping tools are needed and the cycle time can be minimized to save time on the production line. However, the temperature in the tool must be monitored and controlled very precisely and an additional heating furnace and an extra transfer system are needed. Moreover, the dimensional accuracy may not be as high as that obtained with the partitioning method carried out inside the mold.

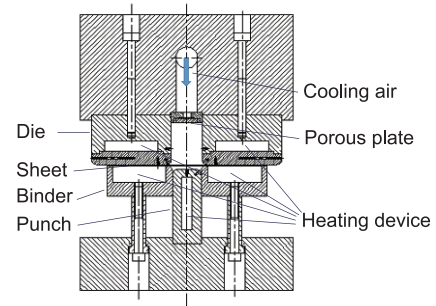


Figure 2 (Color online) Experimental tool design for Q&P hot stamping.

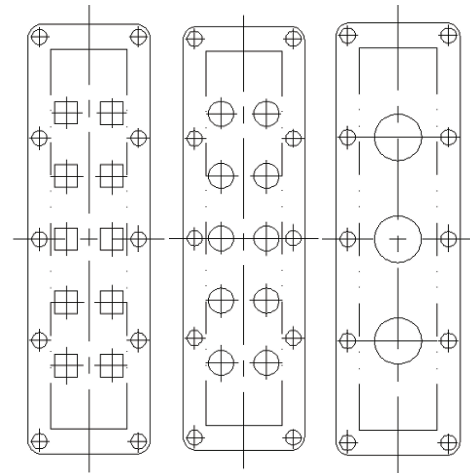


Figure 3 Designs for the porous plate.

3 Hot stamping experiments for a U-cap part

In this section, the Q&P hot stamping process was carried out on an uncoated and cold-rolled steel, B1500HS, produced by BaoSteel Co. B1500HS is a commonly used hot stamping material with a composition of 0.25C-0.22Si-1.29Mn-0.056Al-0.0021B wt.%, which is similar to that of 22MnB5. During the hot stamping experiments, the blank was heated up to 920°C and held at that temperature for 5 min to ensure that the steel fully austenitized. It was then transferred quickly to the stamping tool as described above to successively perform the forming, quenching, and partitioning processes. Then, the formed part was removed from the tool and quenched to room temperature using water. To study the effects of the quenching temperature and partitioning time, T_Q was varied to 350, 300 or 250°C with $t_p=80$ s, and t_p was varied to 40, 80, or 120 s with $T_Q=350$ °C. Conventional hot stamping was also performed in the same tool to compare the results of these two processes. The formed part was kept inside the cool tool until it reached room temperature following both processes.

The final part is shown in Figure 4(a), and its dimensions

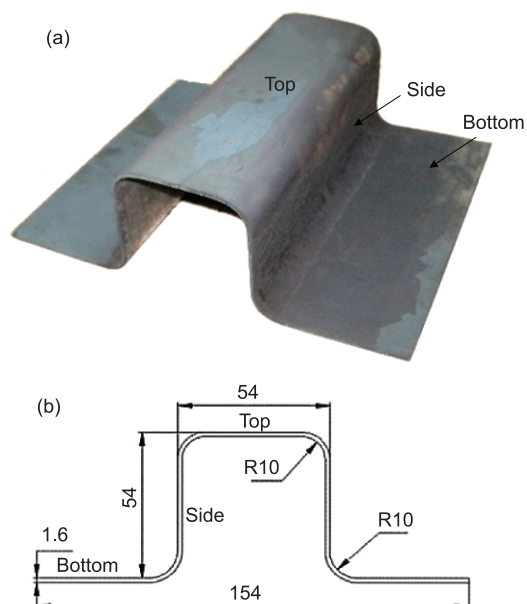


Figure 4 (Color online) Experimental part. (a) The produced part; (b) a dimensional drawing of the part.

are defined in Figure 4(b). According to the geometrical properties of the part, three characteristic regions were examined: bottom, middle, and top. The tensile specimens were cut from the centers of these parts, and the tensile tests were performed at room temperature.

Figure 5 presents the mechanical properties measured by the tensile tests, in which HS denotes the conventional hot stamping and HS+Q&P represents the Q&P hot stamping. The results show that the PSPs of most of the samples from the Q&P hot stamping process are better than those from conventional hot stamping. Figure 5(a) shows that different posi-

tions of the part have different mechanical properties. Specifically, the strength of the bottom region is generally higher than the strength in the other regions and the elongation of the top region is higher than that of other regions and the side region properties between those of the other two regions. This observed profile of mechanical properties arises from the contact conditions during the forming process, which affects the temperature variation and influences the microstructure evolution.

It should also be noted that the process parameters used for the conventional hot stamping were optimized for that process and have been used in many studies. However, Q&P hot stamping involves more process parameters and, therefore, facilitates more possibilities for different properties. For the studied U-cap model, the optimized combination of parameters can be identified to yield a better strength and elongation for all positions compared with those of the conventional hot stamping, as shown in Figure 5(b). For example, when $T_Q=350^\circ\text{C}$ and $t_p=40$ s, the PSPs of the top, side, and bottom regions of the Q&P hot-stamped parts reached 13.0, 15.8, and 18.0 GPa%, respectively, which are higher than the corresponding values in the conventionally hot-stamped parts (11.4, 12.8, and 11.4 GPa%).

4 Material selection for the Q&P process

According to previous studies dealing with the hot stamping process and Q&P treatment, several alloying elements are commonly used: carbon (C), manganese (Mn), Silicon (Si), aluminum (Al), and boron (B). A high C content increases the strength and hardness of the steel; further, retained austenite can be stabilized at room temperature only if there is enough

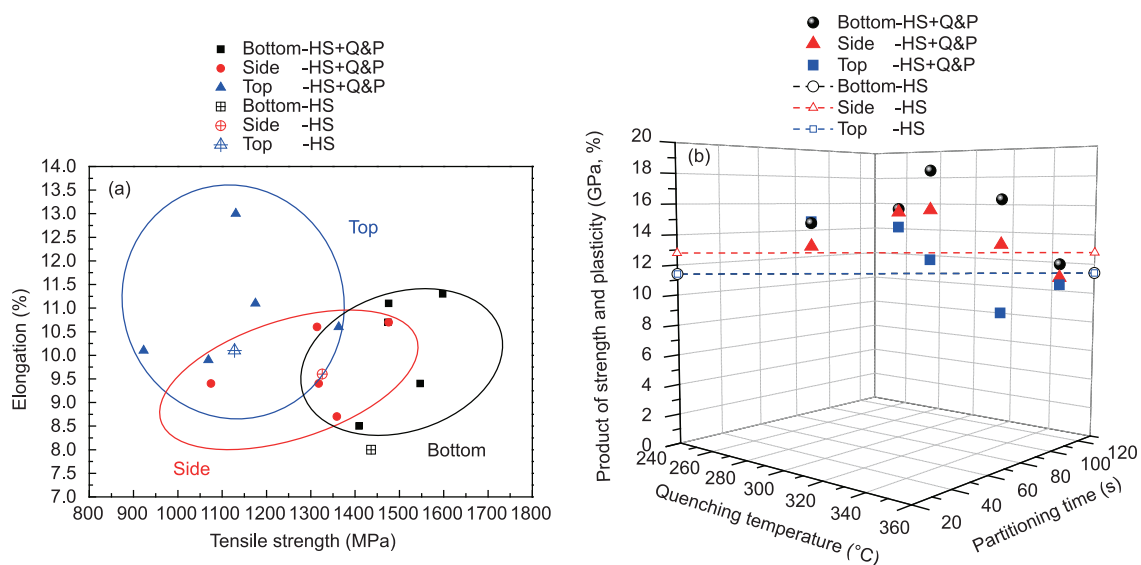


Figure 5 (Color online) Mechanical properties in different regions of the parts produced by the two processes. (a) The strength and elongation; (b) the PSP as a function of the process parameters.

C from martensite available during the partitioning process. However, an excessive C content causes the formation of twin martensite and decreases the ductility and weldability of the steel. The function of Mn is to increase the strength and hardenability of the steel. In the Q&P hot stamping process, Mn decreases the Ms and helps stabilize the retained austenite. Si promotes the diffusion of C from as-quenched martensite to austenite and retards cementite precipitation from these phases, which is important during the partitioning process. Si also helps to strengthen the ferrite phase. The recommended content of Si is higher than 1% for such purposes [29,30], but an excessive Si content decreases the rolling quality and readily induces surface defects. However, the occurrence of these surface defects can be reduced by increasing the Al content, as Al functions like Si but with fewer adverse effects, although its solution-strengthening effect is less significant, as explained in ref. [31]. B is very commonly used in the existing steels used for hot stamping as it pushes the time-temperature transformation TTT curve to the right and effectively increases the hardenability [32]. However, recent research by Mohrbacher [33] demonstrated that B may lead to the formation of intermetallic Fe₂₃(C,B)₆ particles that precipitate on the grain boundaries at lower austenite temperatures, which negatively impacts the final properties.

By considering the functions of these basic elements, three mass-produced steels were selected to test the Q&P hot stamping process in this study: B1500HS, 27SiMn, and TRIP780. The chemical compositions of these materials are shown in Table 1.

B1500HS as a commonly used hot stamping steel as discussed above. TRIP780 is a common transformation-induced-plasticity steel, and 27SiMn is usually used as a structural alloy steel. Both TRIP780 and 27SiMn are normally formed at room temperature and are not regarded as hot stamping steels. However, based on Table 1, they have higher concentrations of Si than the hot stamping boron steel, B1500HS, which is important to promote C diffusion in the Q&P process. It should also be noted in Table 1 that

TRIP780 has a lower concentration of B than B1500HS, while 27SiMn has very little B. So, this set of samples also offers an opportunity to test the effects of B in the Q&P process. In addition, the chemical composition of 27SiMn is close to that of TRIP780, but 27SiMn is generally less expensive than TRIP780 and B1500HS.

Figure 6 displays the temperature-phase diagrams and continuous-cooling transformation CCT diagrams for the three steels, which were created using a commercial software package, Jmat-pro 4.1. Based on Figure 6, the austenite transformation temperature is 810°C for B1500HS, 844°C for TRIP780, and 856°C for 27SiMn. The Ms is 387°C for B1500HS, 374°C for TRIP780, and 350°C for 27SiMn, and the martensitic transformation 90%-completion temperature is 273°C for B1500HS, 259°C for TRIP780, and 234°C for 27SiMn (as a reference, the martensitic transformation 100%-completion temperature, Mf, for B1500HS is 235°C according to the experimental results presented by He [34]). Further, the critical cooling rates for the martensitic transformation are 27°C/s for B1500HS and 70°C/s for both TRIP780 and 27SiMn. Evidently, the lack of B affects the critical cooling rate; hence, a higher cooling rate must be provided to ensure a complete martensitic transformation.

A thermal simulation machine, Gleeble3500, was used to perform the Q&P process for these steels. To focus on the effects of the heat treatment and eliminate the influence of plastic deformation, the forming process was not conducted in these experiments. According to the material properties of the steels presented above, the scheme of the thermal simulation was designed, as shown in Figure 7. The three steels were heated to 900°C and held at that temperature for 5 min to allow them to be fully austenitized. T_Q was defined separately for each steel because their Ms and Mf values are different: T_Q values of 350, 320, and 280°C were used for TRIP780, while 350, 300, and 250°C were used for B1500HS and 27SiMn. The t_p values used for all three steels were 10, 40, 80, and 120 s. As the critical cooling rates for the steels vary widely, the cooling rates in Gleeble3500 were set to 30°C/s for B1500HS and 70°C/s for both TRIP780 and 27SiMn. In addition, for the purpose of comparison, full martensitic transformations were carried out wherein only one quenching process was included, the partitioning process was ignored, and the applied cooling rates were 30°C/s for B1500HS and 70°C/s for both TRIP780 and 27SiMn.

Table 1 Chemical compositions (wt.%) of three steels

Material	B1500HS	TRIP780	27SiMn
C	0.245	0.19	0.207
Si	0.22	1.38	1.4
Mn	1.29	1.68	1.28
Al	0.056	0.053	0.06
B	0.0021	0.0015	–
S	0.02	0.0024	0.003
P	0.022	0.012	0.019
Cr	0.174	0.021	–
N	0.19	0.028	0.079
Mo	0.002	–	–

5 Results and discussion

5.1 Mechanical properties

After the Q&P treatments with various parameters, the mechanical properties of the samples were measured. The strength, elongation, and PSP are plotted in Figure 8 and listed in Table 2. The results demonstrate that the strength

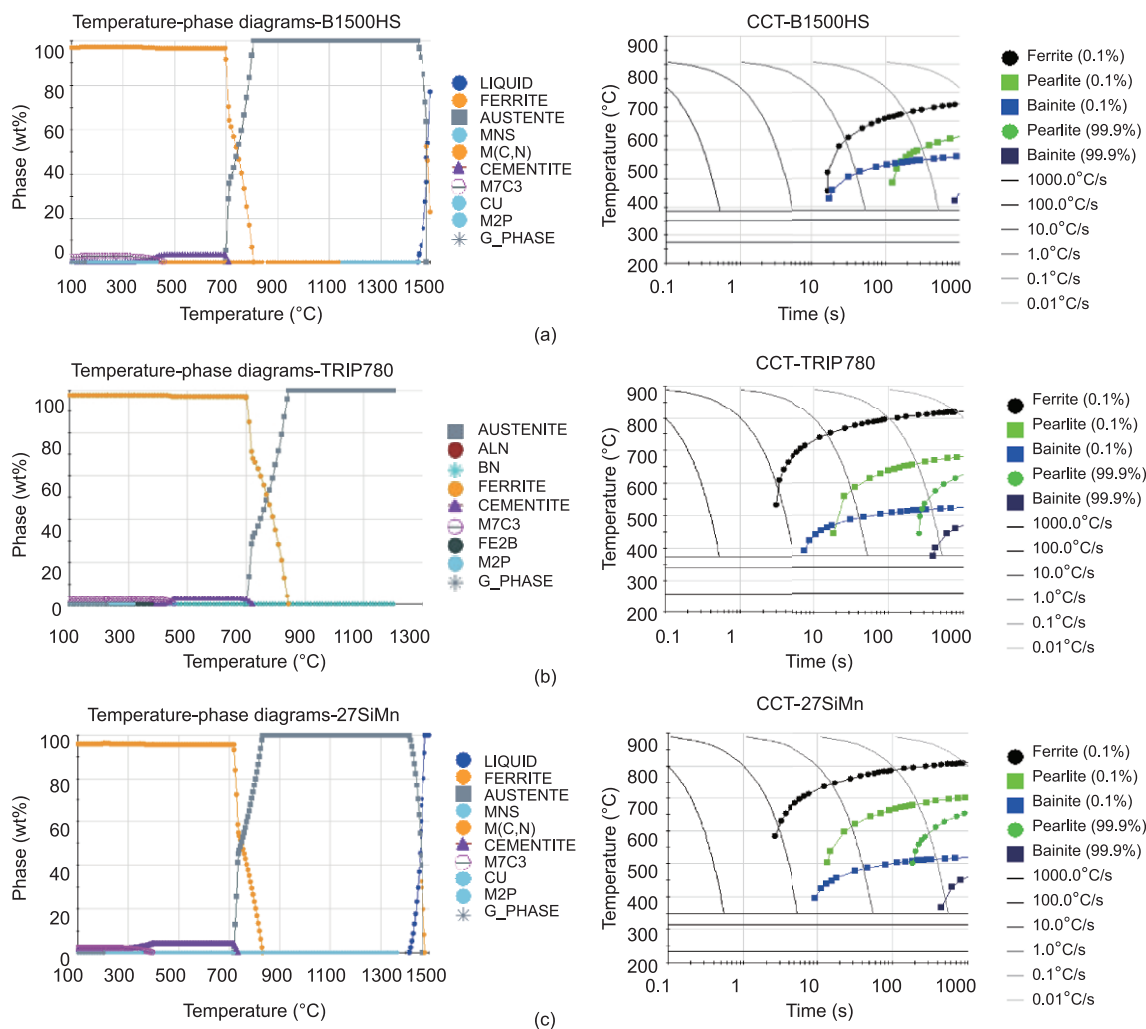


Figure 6 (Color online) Temperature-phase diagrams and CCT diagrams for B1500HS (a), TRIP780 (b), and 27SiMn (c).

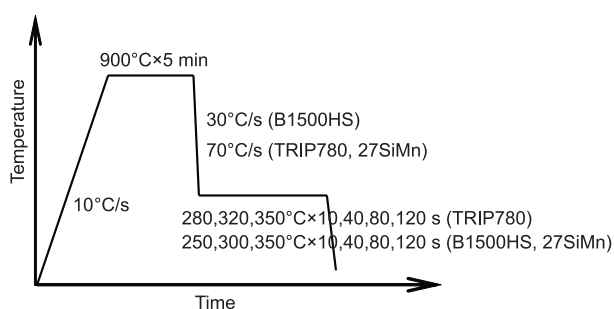


Figure 7 Thermal simulation scheme of the Q&P treatment for the three steels.

range of 27SiMn is higher than those of TRIP780 and B1500HS, while the elongation range of TRIP780 is higher those of 27SiMn and B1500HS. Overall, the PSP values of TRIP780 are generally better than the PSP values of the other steels.

Based on the PSP results, the optimal parameters are adopted as follows: $T_Q=300^\circ\text{C}$ and $t_P=40\text{ s}$ for B1500HS; $T_Q=300^\circ\text{C}$ and $t_P=120\text{ s}$ for 27SiMn; and $T_Q=350^\circ\text{C}$ and

$t_P=120\text{ s}$ for TRIP780. These optimal PSPs, strengths, and elongations of the three Q&P hot-stamped steels are compared with those of the unmodified steels and the samples that underwent the full martensitic transformation, which corresponds to the conventional hot stamping process. As shown in Figure 9, the strengths of these steels increased markedly after the full martensitic transformation, but the elongations decreased, limiting the comprehensive performances (PSPs) of these steels. In contrast, the strengths of the steels after the Q&P process were close to those of the full martensitic transformation but the elongations of the Q&P steels were notably higher in comparison. Thus, the PSPs after the Q&P process are much better than those after the full martensitic transformation. Specifically, the PSP of B1500HS after the Q&P process reached 21.0 GPa%, which is 42.9% higher than that of the original sheet and 144.2% higher than that of the sample that underwent a full martensitic transformation. The PSP of 27SiMn after the Q&P process reached 22.7 GPa%, which is 48.4% higher than that of the original sheet and 164.0% higher than that of the sample that underwent a

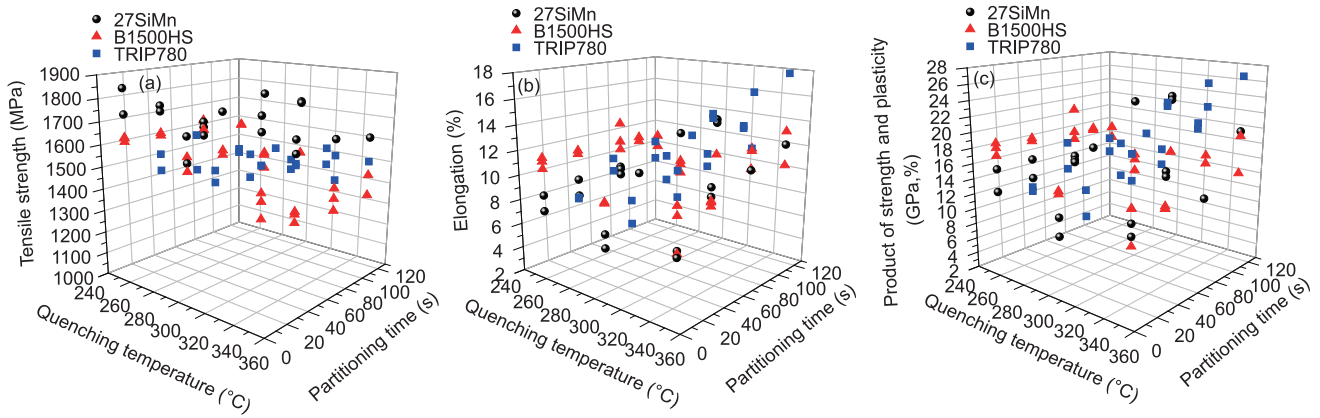


Figure 8 (Color online) Mechanical properties of the three steels as a function of the Q&P parameters. (a) Strength; (b) elongation; (c) PSP.

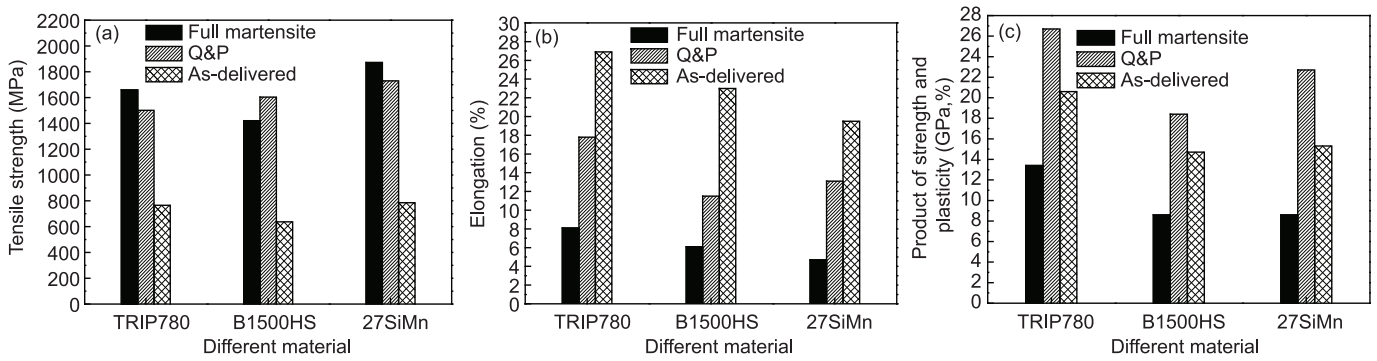


Figure 9 Mechanical properties of steels before and after different processes. (a) Strength; (b) elongation; (c) PSP.

Table 2 Mechanical properties of the three steels

Steel	σ_b (MPa)	A_t (%)	$\sigma_b A_t$ (GPa%)
B1500HS	1390–1624	8.4–13.2	12.7–21.0
TRIP780	1482–1637	8.9–17.8	13.9–26.7
27SiMn	1612–1803	6.2–13.1	10.1–22.7

full martensitic transformation. The PSP of TRIP780 after the Q&P process reached 26.7 GPa%, which is 29.6% higher than that of the original sheet and 99.3% higher than that of the sample that underwent a full martensitic transformation.

The effects of partitioning time, t_p , when $T_Q=350^\circ\text{C}$ are shown in Figure 10. The results show that the strengths of these metals decreased as t_p increased, but the ranges of these changes were small. Taking TRIP780 as an example, the strength dropped 8.3% from 1637 to 1501 MPa. While the elongations increased evidently as t_p increased, for TRIP780 as an example, the elongation increased 49.6% from 11.9% to 17.8%. As the increase of elongation was much larger than the decrease of strength, the PSP generally increased as t_p increased. It is also noted that when t_p was higher than 80 s, the elongation and PSP of B1500HS began to decrease, unlike TRIP780 and 27SiMn. As discussed above, B1500HS lacks Si and therefore lacks the ability to prevent cementite precipitation from the martensite and austenite phases, espe-

cially with a long t_p . This mechanism will be discussed in the following section using scanning electron microscopy (SEM) observations.

The effects of T_Q on the PSP are shown in Figure 11. The effects on the PSPs of TRIP780 and 27SiMn are relatively evident. For TRIP780, the best PSPs were attained when $T_Q=350^\circ\text{C}$ for all values of t_p . The optimal PSP for 27SiMn was attained when $T_Q=300^\circ\text{C}$ except for when $t_p=10$ s; however, this case may be ignored since the PSPs were small under this short partitioning time. However, a clear trend in the effect of T_Q on the PSP of B1500HS was not evident. The optimal T_Q values were different for each t_p , which implies that some unexpected microstructure changes occurred in B1500HS during the Q&P process in addition to the carbon partitioning from martensite to retained austenite.

5.2 Microscopic mechanism

5.2.1 Microstructure observation

Figure 12 shows metallographic images of B1500HS after a full martensitic transformation and following the Q&P treatment. The lath-shaped martensite shown in Figure 12(a) is characteristic of a full martensitic transformation. For the Q&P process with $T_Q=350^\circ\text{C}$ and $t_p=80$ s, the sizes of martensite remained almost unchanged compared with those of the martensite after full martensitic transformation but had white

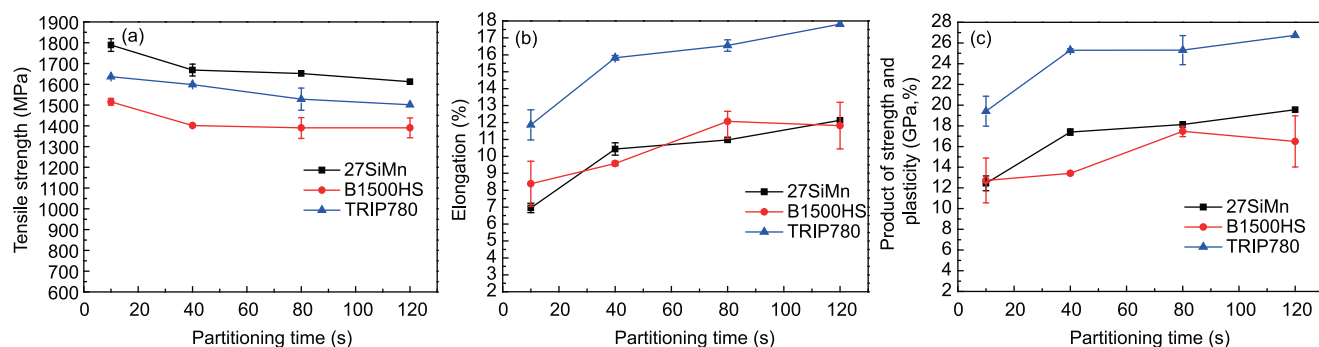


Figure 10 (Color online) Mechanical properties after the Q&P process as a function of the t_p . (a) Strength; (b) elongation; (c) PSP.

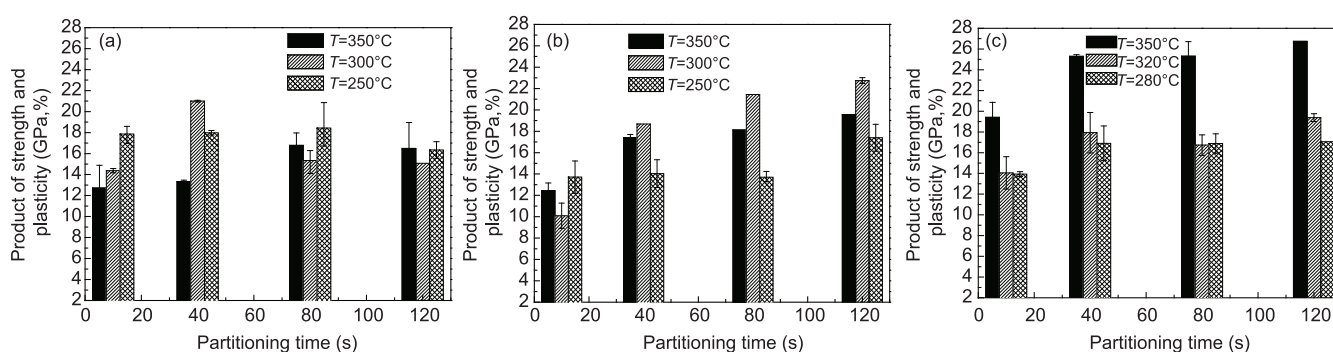


Figure 11 PSPs after Q&P process with different T_Q . (a) B1500HS; (b) 27SiMn; (c) TRIP780.

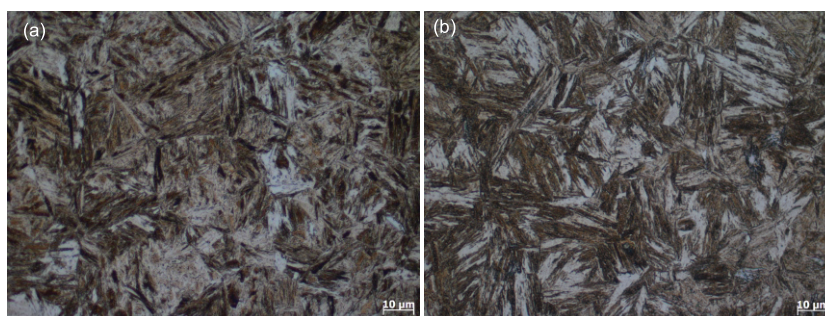


Figure 12 Metallographic structure of B1500HS after a full martensitic transformation (a) and the Q&P process (b).

austenite between the martensitic structures as illustrated in Figure 12(b). A change in the austenite content was also detected by XRD measurements, as shown in Table 3.

During the partitioning process, C atoms migrate from martensite to austenite, which makes the austenite phase rich in C and stable at room temperature. Thus, the final structure of B1500HS after Q&P treatment is composed of both martensite and austenite. The martensite structure provides the required high strength, and the austenite structure offers good deformability and TRIP effects to release local stress concentrations. Such composite microstructures offer advantageous comprehensive mechanical properties.

The optical microscopy observations of TRIP780 and 27SiMn reveal similar structures to that of B1500HS and are not shown here due to space limitations. However, the differences between these steels after the Q&P process can

Table 3 Austenite contents of three steels following different treatments

Steel	Austenite content(%)	
	Full martensitic transformation	Q&P process
B1500HS	1.2	4.7
TRIP780	3.2	9.5
27SiMn	0.12	1.87

be observed in the SEM images in Figure 13, in which $T_Q=350^\circ\text{C}$ and $t_p=80$ s. As shown in Figure 13(a) for B1500HS, a large number of white grains approximately 0.1 μm in diameter were distributed and dispersed in the martensite matrix, which were identified as cementite. The ductility of cementite is extremely poor and its presence decreases the elongation and PSP of the material, as shown

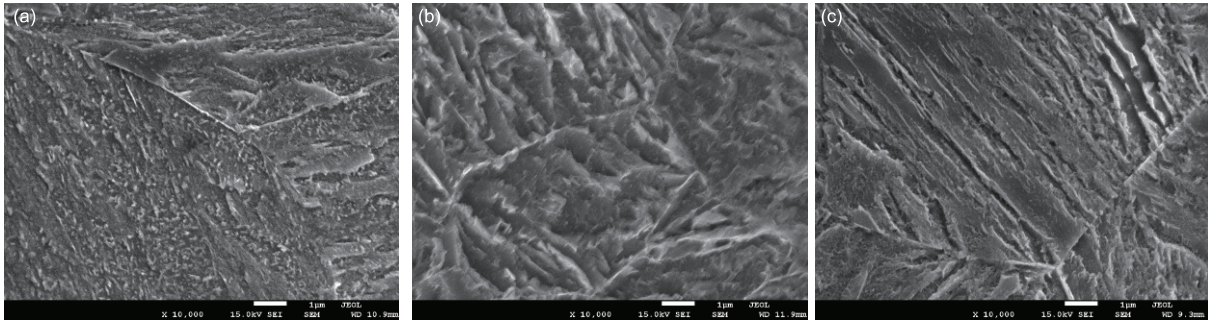


Figure 13 Scanning electron microscopy images after Q&P process. (a) B1500HS; (b) TRIP780; (c) 27SiMn.

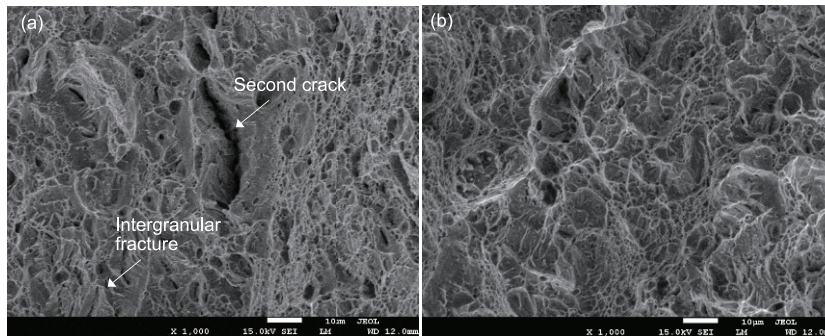


Figure 14 Morphology of the tensile-fracture surface of 27SiMn after a full martensitic transformation (a) and the Q&P process (b).

in Figure 10. Transitional ϵ -carbide precipitates from martensite and tends to transition to relatively stable cementite during the partitioning process. However, Si can retard the formation and growth of cementite. As shown in Figure 13(b) and (c), no obvious cementite can be observed in TRIP780 or in 27SiMn, which contain high concentrations of Si.

5.2.2 Fracture appearance

Tensile tests were performed at room temperature with a crosshead speed of 1 mm/min using a Zwick/Roell Z100 material-testing machine. The samples were cut from the thermal test pieces described above. Figure 14 presents the fracture appearances of samples that underwent a full martensitic transformation those that were Q&P treated with $T_Q=350^\circ\text{C}$ and $t_p=80$ s.

Figure 14(a) shows that the fracture surface of the sample which underwent a full martensitic transformation appears inhomogeneous, indicating a combination of both brittle fracture and ductile fracture. Most of the surface shows features of ductile fracture with the presence of dimples, the sizes of which are generally small and greatly vary. However, the brittle fracture can also be observed in the left part of the surface shown in Figure 14(a), where the fracture started along the grain interface in the form of an intergranular fracture. In addition, long secondary cracks appear in Figure 14(a).

The tensile-fracture surface of the Q&P hot-stamped sample exhibited typical ductile fracture appearance, as shown in Figure 14(b), with dimples which are larger than those in Figure 14(a). This indicates that the ductility of 27SiMn after

the Q&P process is better than that after the full martensitic transformation.

The fracture appearances of B1500HS and TRIP780 were similar to those of 27SiMn.

6 Conclusions

The Q&P hot stamping process for UHSS was further developed in this study. Here, an experimental U-cap stamping tool was developed to perform the forming process. Three widely used UHSS sheet metals were compared in terms of their microstructures and mechanical properties after the Q&P process. The key conclusions are summarized as follows.

(1) Q&P hot stamping technology, which integrates a Q&P heat treatment into the conventional hot stamping process, can be used to produce sheet-metal parts with improved ductility. The microstructure of the material after Q&P hot stamping is composed of martensite and austenite phases.

(2) If the typical boron steels designed for conventional hot stamping, such as B1500HS and 22MnB5, are used for Q&P hot stamping, cementite may appear during the partitioning process, which is likely to decrease the comprehensive properties at higher partitioning times. 27SiMn and TRIP780 are not usually used with hot stamping, but thermal simulation experiments show that both steels can be used in the hot stamping process. Moreover, the performances of 27SiMn and TRIP780 after the Q&P process are better than that of B1500HS. The main reason is that both materials are rich in

Si, which can reduce the formation and growth of cementite.

(3) A U-cap part was fabricated using the experimental stamping tool. Based on the mechanical testing results, the PSP value of the formed region of boron steel can reach 18.0 GPa% with a strength of 1598 MPa and an elongation of 11.3%, the PSP is 57.9% higher than that of the conventionally hot-stamped sample. The key advantage of this Q&P hot stamping tool is that the cooling in quenching stage and temperature holding during the partitioning stage are balanced. The present tool only works for boron steels such as B1500HS for which the critical cooling rate can be attained relatively easy. Further research is necessary to achieve the higher cooling rates needed for the quenching stage for materials that lack boron, such as TRIP780 and 27SiMn.

This work was supported by the National Natural Science Foundation of China (Grant Nos. 51105247 & U1564203).

- 1 Karbasian H, Tekkaya A E. A review on hot stamping. *J Mater Processing Tech*, 2010, 210: 2103–2118
- 2 Hu P, Ma N, Liu L, et al. *Theories, Methods and Numerical Technology of Sheet Metal Cold and Hot Forming*. London: Springer-Verlag, 2013. 35–46
- 3 Geiger M, Merklein M, Hoff C. Basic investigations on the hot stamping steel 22MnB5. *AMR*, 2005, 6-8: 795–804
- 4 Han X, Zhong Y, Yang K, et al. Application of hot stamping process by integrating quenching & partitioning heat treatment to improve mechanical properties. *Procedia Eng*, 2014, 81: 1737–1743
- 5 Rossini M, Spina P R, Cortese L, et al. Investigation on dissimilar laser welding of advanced high strength steel sheets for the automotive industry. *Mater Sci Eng-A*, 2015, 628: 288–296
- 6 Vandeputte S, Vanderschueren D, Classens S, et al. Modern steel grades covering all needs of the automotive industry. In: *Proceedings of Ninth International Conference on Steel Sheet Metal*. Leuven, 2001. 405–414
- 7 Ying S, Dong H. The third generation auto sheet steel: Theory and practice. In: *Proceedings of the FISITA 2012 World Automotive Congress*. Berlin, 2013. 933–947
- 8 Naderi M, Abbasi M, Saeed-Akbari A. Enhanced mechanical properties of a hot-stamped advanced high-strength steel via tempering treatment. *Metall Mat Trans A*, 2013, 44: 1852–1861
- 9 Ying L, Chang Y, Hu P, et al. Influence of low tempering temperature on fracture toughness of ultra high strength boron steel for hot forming. *Adv Mater Res*, 2010, 146-147: 160–165
- 10 Naderi M, Ketabchi M, Abbasi M, et al. Semi-hot stamping as an improved process of hot stamping. *J Mater Sci Tech*, 2011, 27: 369–376
- 11 Naderi M, Ketabchi M, Abbasi M, et al. Analysis of microstructure and mechanical properties of different high strength carbon steels after hot stamping. *J Mater Process Tech*, 2011, 211: 1117–1125
- 12 Santofimia M J, Nguyen-Minh T, Zhao L, et al. New low carbon Q&P steels containing film-like intercritical ferrite. *Mater Sci Eng-A*, 2010, 527: 6429–6439
- 13 Hao L, Xiao N, Zheng C, et al. Mechanical properties and temper resistance of deformation induced ferrite in a low carbon steel. *J Mater Sci Tech*, 2010, 26: 1107–1113
- 14 Speer J, Matlock D K, De Cooman B C, et al. Carbon partitioning into austenite after martensite transformation. *Acta Mater*, 2003, 51: 2611–2622
- 15 Speer J G, De Moor E, Clarke A J. Critical assessment 7: Quenching and partitioning. *Mater Sci Tech*, 2015, 31: 3–9
- 16 Hsu T Y, Jin X J, Rong Y H. Strengthening and toughening mechanisms of quenching-partitioning-tempering (Q-P-T) steels. *J Alloys Compd*, 2013, 577: S568–S571
- 17 Chen M M, Wu R M, Liu H P, et al. An ultrahigh strength steel produced through deformation-induced ferrite transformation and Q&P process. *Sci China Technol Sci*, 2012, 55: 1827–1832
- 18 Liu H, Jin X, Dong H, et al. Martensitic microstructural transformations from the hot stamping, quenching and partitioning process. *Mater Charact*, 2011, 62: 223–227
- 19 Liu H, Lu X, Jin X, et al. Enhanced mechanical properties of a hot stamped advanced high-strength steel treated by quenching and partitioning process. *Scripta Mater*, 2011, 64: 749–752
- 20 Han X, Zhong Y, Xin P, et al. Research on one-step quenching and partitioning treatment and its application in hot stamping process. *Proc Institution Mech Engineers Part B-J Eng Manufacture*, 2015, 84: 163–182
- 21 Han X, Xin P, Hao X, et al. A new try of hot stamping process with higher strength-ductility balance. In: *Proceedings of International Deep Drawing Research Group IDDRG*. Zurich, 2013. 659–669
- 22 Lin T, Song H W, Zhang S H, et al. Microstructure, mechanical properties, and toughening mechanisms of a new hot stamping-bake toughening steel. *Metall Mat Trans A*, 2015, 46: 4038–4046
- 23 Santofimia M J, Zhao L, Petrov R, et al. Characterization of the microstructure obtained by the quenching and partitioning process in a low-carbon steel. *Mater Charact*, 2008, 59: 1758–1764
- 24 Paravicini Bagliani E, Santofimia M J, Zhao L, et al. Microstructure, tensile and toughness properties after quenching and partitioning treatments of a medium-carbon steel. *Mater Sci Eng-A*, 2013, 559: 486–495
- 25 Li H Y, Lu X W, Wu X C, et al. Bainitic transformation during the two-step quenching and partitioning process in a medium carbon steel containing silicon. *Mater Sci Eng-A*, 2010, 527: 6255–6259
- 26 Zhao H S, Li W, Zhu X, et al. Analysis of the relationship between retained austenite locations and the deformation behavior of quenching and partitioning treated steels. *Mater Sci Eng-A*, 2016, 649: 18–26
- 27 Zhong N. *Research on High Strength Q&P and Q-P-T Steels*. Dissertation for Doctoral Degree. Shanghai: Shanghai Jiao Tong University, 2009. 139
- 28 Han X, Cui Z, Xin P, et al. A U-shape tool design for one-step Q&P hot stamping process. *China Patent*, ZL 201310335789.1, 2015-05-20
- 29 Saleh M H, Priestner R. Retained austenite in dual-phase silicon steels and its effect on mechanical properties. *J Mater Process Tech*, 2001, 113: 587–593
- 30 Jacques P, Girault E, Catlin T, et al. Bainite transformation of low carbon Mn-Si TRIP-assisted multiphase steels: influence of silicon content on cementite precipitation and austenite retention. *Mater Sci Eng-A*, 1999, 273-275: 475–479
- 31 Mahieu J, Van Dooren D, Barbé L, et al. Influence of Al, Si and P on the kinetics of intercritical annealing of TRIP-aided steels: Thermodynamical prediction and experimental verification. *Steel Res*, 2002, 73: 267–273
- 32 Haga J, Mizui N, Nagamichi T, et al. Effect of boron on mechanical properties and recrystallization behavior of Ti-added ultra-low carbon cold-rolled steel sheets. *Isij Int*, 1998, 38: 580–586
- 33 Mohrbacher H. Martensitic automotive steel sheet - fundamentals and metallurgical optimization strategies. *Adv Mater Res*, 2014, 1063: 130–142
- 34 He L. *Research on Key Parameter Measuring and Quenching Properties of Boron Steel B1500HS in Hot Stamping Process*. Dissertation for Doctoral Degree. Jinan: Shandong University, 2012